Efficient Electrocatalytic Switching of Azoheteroarenes in the Condensed Phases

Jake L. Greenfield,[a,#] Mihael A. Gerkman,[b,#] Rosina S. L. Gibson,[a] Grace G. D. Han,[b,*] and Matthew J. Fuchter[a,*]

[a] Molecular Sciences Research Hub, Department of Chemistry, Imperial College London, London W12 0BZ, U.K.

[b] Department of Chemistry, Brandeis University, Waltham, Massachusetts 02453, USA

[#] *These authors contributed equally*

Supporting Information Placeholder

ABSTRACT: Azo-based photoswitches have shown promise as molecular solar thermal (MOST) materials, due to their ability to store energy in their metastable *Z* isomeric form. The energy is then released, in the form of heat, upon photoisomerisation to the thermodynamically stable *E* form. However, obtaining a high energy density and recovering the stored energy with high efficiency requires the materials to be employed in the condensed phase and display a high degree of *Z* to *E* switching, respectively: both of which are challenging to engineer. Here we show that arylazopyrazole motifs undergo efficient redox-induced *Z* to *E* switching in both the solution and condensed phase, to a higher completeness of switching than achieved photochemically. This redox-initiated pathway lowers the barrier to *Z* to *E* isomerization by 27 kJ/mol, whilst in the condensed phase, the efficiency of electrochemical switching is improved by over an order of magnitude relative to that in the solution state. The influence of the photoswitch's phase, electrical conductivity, and viscosity on the electrochemical switching in the condensed phase is reported, culminating in a set of design rules to facilitate further investigations. We anticipate the use of an alternative stimulus to light will facilitate the application of MOST materials in situations where photo-triggered heat release is unachievable or inefficient, e.g. indoor or at night. Furthermore, exploiting the electrocatalytic mechanism, whereby a catalytic amount of charge triggers *Z* to *E* switching via a redox process, bypasses the need for fine-tuning of the photoswitching chromophore to achieve complete *Z* to *E* switching, thus providing an alternative approach to photoswitch molecular design.

Introduction

The ability of photoswitches to effectively store, as well as release, solar energy has rendered them ideal candidates in the development of molecular solar thermal (MOST) materials.[1] These include norbornadienes,[2–6] dihydroazulenes,[7] and azobenzene[1,8–10] based photoswitches as well as fulvalene diruthenium based complexes.[11] Of the photoswitches, those containing azo-linkages have been championed for their low cost, ease of synthesis and derivatization, and cycle stability.[1] To date, significant strides have been made towards improving the figures of merit of azo-based MOST materials, notably the expansion of the energy storage density.[1] However, several properties still require addressing, including, maximizing the completeness of bidirectional switching, prolonging the thermal half-life of the metastable state, demonstrating the energy storage in condensed phases, and developing new strategies of user-controlled heat release.[1,12]

To date, energy release from azobenzene-based MOST compounds has been performed via optically triggering the *Z* to *E* isomerization process,[13] however, there are circumstances where photoinduced heat release is ineffective and incomplete. This includes usage in regions/applications displaying low-light intensity, for example, their usage at night or indoors. In addition, many azo-based MOST compounds possess poor optical properties, resulting in incomplete reverse isomerization at the photostationary state (PSS).[1,14] In particular, some of the recently developed azoarene switches, which display superb thermal stability, e.g. *o*-fluoroazobenzene derivatives[15] and 4PzH,[13,14,16,17] display incomplete photo-induced reverse isomerization. Complete photoinduced *Z* to *E* isomerization mostly requires a large separation of the optical absorption bands between the two isomeric states, achieved through the judicious design of the switch's chromophore.[14] However, such an optimization of the chromophore is often compromised by a lowered energy density.[1,18] This is illustrated by the *ortho*-functionalized azobenzene derivatives that exhibit a significant separation between n–π* bands of *E* and *Z* isomers (hence better bidirectional switching),[18,19] but much lower isomerization energy (20-30 kJ/mol)[18–20] compared to the pristine azobenzene (41.4 kJ/mol).[21] Alternative triggering methods to return to the thermodynamically stable state[22] include thermal activation[13] and metal-oxide-driven catalysis,[2,3,23] typically utilized for azoarenes and norbornadienes, respectively. Thermal reversion typically requires substantial energy input to overcome the activation barriers for the azoarene *Z* to *E* isomerization, in the range of 100-133 kJ/mol ($\Delta H^{\ddagger}$),[14,16,24,25] and high-temperature conditions ranging from 70 to 120 °C depending on the structure of the photoswitch.[14,16] Alternatively, the use of chemical and photoredox catalysis to trigger *Z* to *E* isomerization has emerged as another tool to lower the activation energy,[26,27] largely focused on the norbornadiene derivatives.[28–31] Thus, investigations into

alternative stimuli to induce *Z* to *E* switching may further expand the opportunities[32–35] available to the azoarenes and increase the efficiency of triggered heat release.[12]

Recently, the groups of Hecht and Saalfrank reported electrochemically-induced *Z* to *E* switching of azobenzene derivatives under both oxidizing[26] and reducing[27] conditions in solution. In addition to achieving complete *Z* to *E* isomerization using an orthogonal stimulus to light irradiation, their results are particularly interesting since the electrochemically-induced switching was shown to be electrocatalytic: only a substoichiometric number of electrons, or holes, were required to drive the *Z* to *E* switching process to completion.[26] In principle, this approach holds great promise as a useful feature for energy storage,[28] where a catalytic trigger may allow for favorable energy balance in the process. However, much remains unknown about electrochemical switching of azoarene photoswitches, and particularly if it is possible to translate the facile electrocatalytic switching into the condensed phase where conformational changes[36] have been observed to be significantly hindered.[37,38]

While many of the azo-based energy storage materials have focused on azobenzene derivatives, we[13] and others[17,39] have recently shown arylazopyrazole switches[14] to hold particular promise as MOST materials, given the excellent thermal stability (4PzH-F2 (compound **S7** in Supporting Information): $t_{1/2}$ ~46 years)[16] of their *Z*-isomer and ability to control phase transitions.[13] Despite having a moderate energy density and the longest *Z* to *E* thermal half-lives reported to date, many arylazopyrazoles exhibit a significantly reduced *Z* to *E* isomerism (42% *E* at the 420 nm PSS, for 4PzH-F2),[13,17] which remains a challenge for the deployment of such materials for solar energy harvesting and heat release applications.[1] Therefore, there is a critical need to develop an alternative triggering method that offers complete and efficient *Z* to *E* switching and subsequent heat release in a condensed phase.[12]

Herein, we report the electrochemical switching behavior of arylazopyrazoles in both solution and condensed phase: before this study, it was not known whether such switches undergo analogous electrochemistry/electrocatalytic switching to azobenzenes.[26,27] Not only do the arylazopyrazoles undergo efficient electrochemical *Z* to *E* switching in solution but this electrochemical switching is efficiently translated to the condensed phase. Through employing thin films, we demonstrate *Z* to *E* electrochemical switching of our materials in a device, noting that the catalytic efficiency of the switching improves by over an order of magnitude in the condensed phase. Through judicious choice of switch design, the material properties that underpin efficient electrochemical switching in the condensed phase are determined. This study serves as a platform for the further development of electrocatalytic azo-based MOST materials for use in energy storage applications.

Results and Discussion

Structural Design. Photoswitches **1**-**3** were synthesized in good yield based on procedures previously reported by Fuchter[13] and Kimizuka, et al. (Figure 1a).[40] These switches were designed to exhibit different physical properties in the condensed phase so that the parameters influencing electrochemical switching in the condensed phase could be decoupled. These parameters include the intrinsic electrical conductivity, viscosity, and phase of the material. We have previously shown that **1**, a candidate for long-term energy storage, exists as a liquid in its *Z* form.[13] We hypothesized that the low viscosity of the liquid *Z* form of **1**, similar to glycerol, might improve its switching ability in the condensed phase, rendering it amenable for use in an electrochemical device. Ionic arylazopyrazole derivatives **2** and **3** were employed to study the influence of the intrinsic film conductivity on the electrochemical switching process. While **2** exists as a solid in its *E* and *Z* form until melted (where both isomers form a stable supercooled liquid down to 0 °C), switch **3** is a room-temperature ionic liquid in both isomeric forms. The thermal properties of photoswitches **1**-**3** are shown in Figure S1, S2 and Table S1.

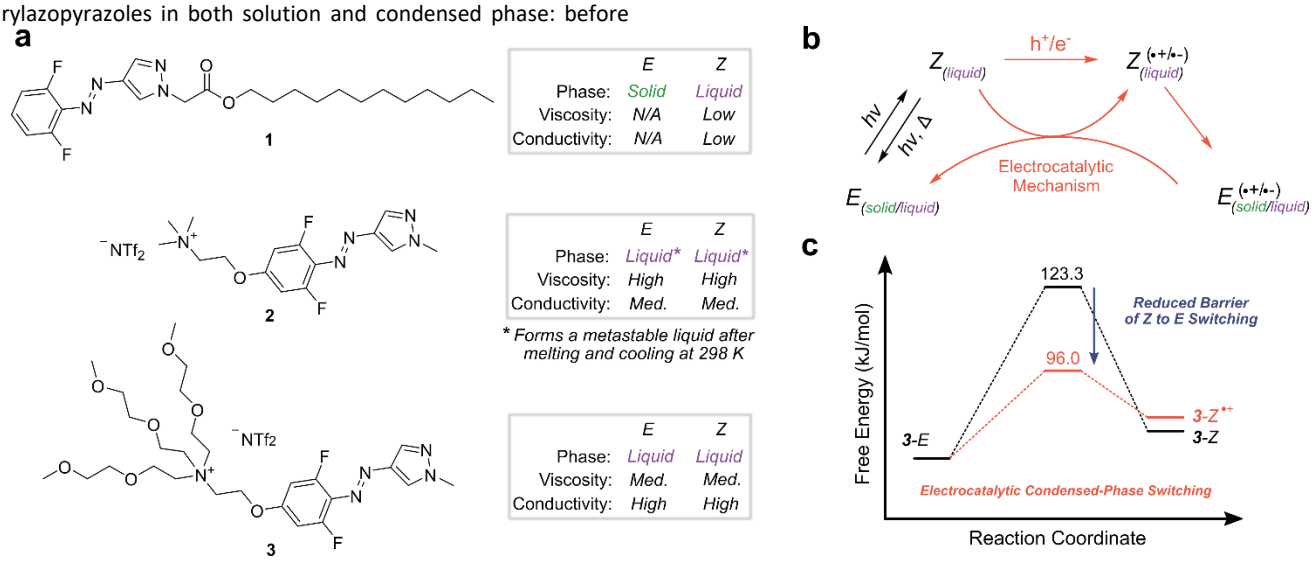


Figure 1. a, Structures of the switches employed in this study. Synthetic details are described in the supporting information. **b**, Schematic of the electrochemically induced electrocatalytic mechanism of *Z* to *E* isomerization. **c**, Energy diagram showing a reduction in the activation energy ($\Delta G^{\ddagger}$) of the *Z* to *E* switching process for the electrocatalytic mechanism compared to thermal reversion at 298 K. This energy reduction corresponds to 27.3 kJ/mol, determined for **3** in the condensed phase using the Eyring equation (Section 3.22 of the Supporting Information).

Table 1. A summary of the photophysical, redox and electrocatalytic properties of switches **1**-**3**.

	%*Z* at PSS[a]										
	340 nm	365 nm	395 nm	495 nm	530 nm	*Z* to *E* Oxidative Switching[b]	$t_{1/2}$ (years)	E_p^a (V)[c]	E_p^c (V)[c]	mol% Charge (*Solution*)[d]	mol% Charge (*Film*)
1	98%[e]	44%	62%	17%	85%	*Quant.*	46[f]	1.49	1.84	8.8	0.7
2	99%	84%	53%	73%	-	*Quant.*	12[g]	1.17	1.91	16.5	2.2
3	98%	89%	55%	76%	-	*Quant.*	14[h]	1.16	1.93	17.5	12.6

Photostationary state (PSS), thermal half-life ($t_{1/2}$) of *Z* isomer at 298 K, anodic peak potential (E_p^a), cathodic peak potential (E_p^c). Max. and min. %*Z* at PSS are marked purple and green, respectively, to indicate the most optimal light sources for photoswitching. [a] Determined using ^{1}H NMR in CD_3CN at 298 K (Section 3.5 of Supporting Information). [b] Determined in the solution state using UV-vis spectroelectrochemical measurements (Section 3.7 of Supporting Information). [c] Determined using cyclic voltammetry in a 0.1 M $TBAPF_6$/MeCN electrolyte at 298 K under Ar, referenced to the Fc/Fc^+ redox couple. [d] Determined from data in Figure 2b. [e] Value previously reported in $CDCl_3$.[13] [f] Value of the previously reported parent compound.[16] [g] Determined using UV-vis kinetic measurements (Figure S14) [h] Determined using ^{1}H NMR kinetic measurements (Figure S16).

Electrochemical Switching: Solution State. We first examined the solution state redox properties of compounds **1-3** and other arylazopyrazole derivatives (Figure S3) using cyclic voltammetry (Figure S4-S6, Table S2). These switches exhibit a quasi-reversible reduction process and an irreversible oxidation process. No discernable differences in the redox potentials of the *E* and *Z* forms of the photoswitch were observed in the cyclic voltammograms. Analogous behavior has been previously reported for azobenzene derivatives,[26,27] attributed to an electrocatalytic process that results in rapid *Z* to *E* isomerism upon either oxidation or reduction of the *Z* isomer (Figure 1b, c). In such cases, DFT investigations were used to probe the relative redox potential of the *Z* isomer, which couldn't be detected using CV, relative to the *E* isomer.[26,27] The studies detailed herein focuses on the oxidative process which requires a lower potential (vs Fc/Fc^+) application compared to the reduction by 0.3-0.8 V. Also, the oxidative pathway does not require inert conditions due to the absence of oxygen reduction side reactions and is therefore more easily translatable to application.[26]

The proposed oxidative electrocatalytic switching mechanism, induced by the formation of the radical cation of the *Z* isomer ($Z^{\bullet+}$), was supported by DFT calculations. Following the approach adopted by Hecht and coworkers,[26] the ionization potentials (IP) of a series of model compounds were determined both in the gas phase and with an acetonitrile PCM solvation model (Table S3). For all compounds investigated, the IP's of the *Z* isomer were consistently obtained at a lower energy than the *E* isomer. Based on this ordering of the IP's of the two isomeric forms, the oxidation potential of the *Z* isomer is expected to be lower than that of the *E*. In addition, the electron transfer process from *Z* to $E^{\bullet+}$, i.e. propagation of the chain reaction, was also found to be energetically favorable (Table S5). The combination of the ionization potential and an energetically downhill electron transfer process support the assignment of an electrocatalytic mechanism.

UV-vis spectroelectrochemical measurements revealed that complete *Z* to *E* isomerism was achieved at potentials lower than that of the anodic peak currents (Section 3.3 and 3.7 of Supporting Information), in agreement with the computational studies (Section 3.4 of Supporting Information). Complete *Z* to *E* conversion of **3** was achieved at 1.00 V (vs. the Fc/Fc^+ redox couple), 0.16 V below the oxidation wave observed in cyclic voltammetry studies (Figure 2a, Table S2). The presence of an isosbestic point indicates clean *Z* to *E* isomerization without detectable degradation. Further oxidation above 1.35 V (vs Fc/Fc^+) afforded irreversible changes in the UV-vis spectrum and loss of the isosbestic point, indicating the decomposition of **3**-$E^{\bullet+}$ (Figure S17). Interestingly, complete *Z* to *E* conversion was observed for switches **1**-**3** (Table 1); such high levels of reversion to the thermodynamically favored isomers were difficult to achieve via direct photoswitching due to the overlap between the absorption spectra of the *E* isomers compared to *Z* (Figure 2a). Since complete *Z* to *E* switching was also achieved upon application of a reductive potential (-1.65 V vs Fc/Fc^+ for **3**, Figure S17), we infer this to be a candidate for the counter redox process for experiments in the absence of an electrolyte (Figure 3). Oxidative *Z* to *E* switching could also be achieved using the molecular oxidizing agent ceric ammonium nitrate (CAN, Figure S21). Surprisingly, complete *Z* to *E* conversion could be achieved upon addition of 30 mol% of CAN to a 40 µM solution of *Z*-**3**, even though the oxidation potential of CAN was measured to be 0.30 V lower than the onset potential of *Z* to *E* switching of **3**. This apparently energetically unfavorable process was rationalized based on the rapid exergonic *Z* to *E* isomerism upon formation of $Z^{\bullet+}$.[26,27]

Despite the thermal half-life of **3** being ca. 14 years at 298 K (Table 1), and the switches' limited photoinduced *Z* to *E* conversion (24% *E* at 495 nm PSS), the *E* form could be obtained quantitatively within minutes at room temperature under the applied anodic potential. This electrochemical switching strategy was further applied to convert a bulk solution of a metastable photoswitch to its thermodynamically favored form: 20 mL of a 2.5 mM solution of *Z*-**3** was converted to *E*-**3** over several hours using a 2.2 cm^2 surface area Pt wire coil working electrode fixed at 1.00 V (vs Fc/Fc^+) with constant stirring (Figure S22). The significant increase in the rate of isomerization for $Z^{\bullet+}$ was also probed computationally. The energy of the transition state of a derivative of **2**-$Z^{\bullet+}$, (**2'**), was determined to be 1.15 eV lower in energy than the transition state of the neutral form *Z* (Table S4). According to the Eyring equation, this corresponds to a 19-order of magnitude difference in the rate of isomerization. With further optimization, such rapid isomerization should alleviate issues with slow heat release and therefore should be beneficial towards increasing the power output of an energy storage material.

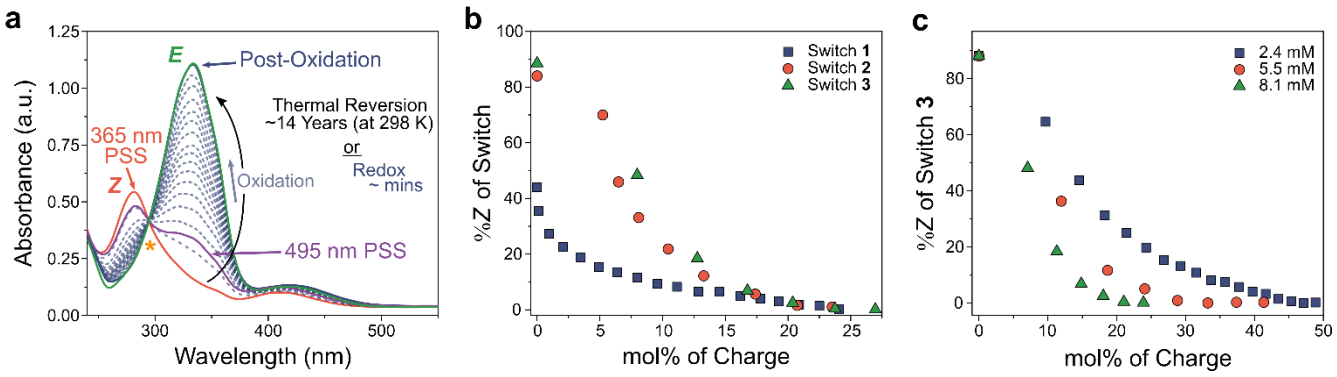


Figure 2. a, Solution state, UV-vis spectrum of photoswitch **3** highlighting the effectiveness of using an oxidative stimulus to trigger *Z* to *E* isomerism compared to photoirradiation and thermal reversion. The measurements were performed at 3 mM in an OTTLE cell containing a 0.5 M $TBAPF_6$ electrolyte. The cell is comprised of a Pt mesh working electrode, a Pt mesh counter electrode, and an Ag wire quasi-reference electrode, which was referenced against the Fc/Fc^+ redox couple. All measurements were carried out at 298 K and the cell was prepared and sealed with PTFE plugs in an inert atmosphere. The orange asterisk indicates the presence of an isosbestic point. **b**, Comparison of the efficiencies of electrochemical conversion for switches **1**-**3**. The "mol% of Charge" was calculated based on the expected number of charges required to oxidize the given sample concentration based on the calibration shown in Figure S24. Solutions used in these measurements comprised of a ca. 8 mM solution of the switch in a 0.5 M $TBAPF_6$ electrolyte, held at a fixed potential (1.35 V for **1**, 1.10 V for **2** and 1.00 V for **3**, vs Fc/Fc^+). **c**, The effect of substrate concentration on the amount of charge required to switch compound **3** from an 88.5% *Z*-rich PSS to the *E*-state. Experiments were carried out in a 0.5 M $TBAPF_6$/MeCN electrolyte solution. The potential was held at 1.00 V vs Fc/Fc^+. The percentage of switching was monitored using the absorption at 281 nm. In both **b** and **c**, the samples were optically switched (365 nm) to a *Z*-rich PSS before oxidation. The calibration procedure to determine the electroactive volume of the cell used in **b**, and **c**, is reported in Section 3.11 of the Supporting Information.

The cycle stability of the electrochemically induced *Z* to *E* switching was measured in solution for **3** (Figure S23). Good stability was observed in the solution state, noting a maximum possible degradation of 14% after 20 cycles. We attribute this to the generation of *E*-$\mathbf{3}^{\bullet+}$ which subsequently degrades (Figure S17). Such degradation may be reduced for switches that display greater electrocatalytic performance.

Efficiency of Electrocatalytic Switching: Solution State. The efficiency of the oxidative electrocatalytic switching in the solution state was gauged using coulometry.[41] An optically transparent thin layer electrochemical (OTTLE) cell was adopted to determine the extent of *Z* to *E* switching as a function of the number of charges injected into the system.[41] The efficiency of the hole-induced electrocatalysis in the solution state for switches **1**-**3** is presented in Figure 2b. The mol% of charge was determined based on the concentration of the photoswitch and the number of charges required to oxidize the *Z* isomer (Figure S24-S25). It is evident that a substoichiometric number of charges, less than 25%, are required to induce the complete conversion of a *Z*-rich PSS to the *E* isomer. Fitting the initial points of each data set linearly, thus reducing the contributions of diffusion of material to the working electrode,[41] the efficiency of solution-state switching was estimated to be highest for **1**: only 8.8 mol% of charge was required to switch **1** from *Z* to *E* (Table 1). Compounds **2** and **3** require a similar number of charges (16.5-17.5 mol%) to undergo complete *Z* to *E* switching. Moreover, the efficiency of the electrocatalytic switching is discovered to be dependent on the concentration of the photoswitch (Figure 2c). Increasing the concentration of compound **3** results in a more efficient switching process, requiring fewer charges to achieve complete switching. Specifically, increasing the concentration from 2.4 mM to 8.1 mM reduces the number of charges required to achieve switching by a factor of *ca.* 2. We infer this to be due to the photoswitches being in closer proximity, thus increasing the local concentration of the *Z* isomer and disfavoring deactivation processes that may lead to termination of the propagating species.[26] Given the improved efficiency of the electrocatalytic reaction at higher concentrations, we hypothesized that further improvements might be obtained in the condensed phase.

Electrochemical Switching: Condensed Phase. To test this hypothesis, thin films of switches **1**-**3** were prepared on conductive ITO-coated glass substrates based on the device architecture shown in Figure 3a. Details regarding the fabrication of these devices are reported in Section 1.1 of the Supporting Information. The photoswitches were deposited on the ITO surface in the liquid state: at room temperature, **1**-*Z* exists as a liquid[13] and **3** exists as a liquid in both isomeric forms. For **2**, the *E* and *Z* isomers melt at 124 and 96 °C, respectively. However, once melted, **2** exhibits behavior consistent with a super-cooled liquid, existing in a metastable liquid down to 0 °C (Figure S2). The electrical conductivities of these films were measured with a conductivity meter (Figure S27, Table S7): **3**-*Z* displayed the greatest conductivity, reaching values as high as 8.6 µS/cm at 25 °C, 3 orders of magnitude larger than **1**-*Z* (0.004 µS/cm). This relatively high value was attributed to its ionic-liquid properties whereby its ionic nature provides a higher density of charge carriers, whilst its liquid phase behavior facilitates charge migration in response to an applied electric field (Figure S28). Compound **2**-*Z*, a super-cooled ionic liquid, exhibited an intermediate conductivity, 0.086 µS/cm.

The light penetration depth of a film containing **3** was estimated using the approach detailed by Grossman and co-workers (Figure S29).[9] A penetration depth of 1 µm was determined for *E*-**3** at 340 nm of incident light, which increases to over 400 µm for *Z*-**3,** as the *E* to *Z* conversion gradually occurs. Thus, the films employed in this study, 10-25 µm, are able to be effectively converted to their *Z*-form under UV irradiation. From this analysis, it is found that films thicker than 400 µm will lose efficiency of photoswitching and require mixing of *E* and *Z* mixtures to increase the exposure of *E* to UV light.

A key consideration that dictates the ability for photoswitches to undergo a change in geometry (*E*/*Z* isomerization) in the condensed phase is the steric hindrance imposed by the dense packing of molecules and the absence of solvation.[37] We investigated this aspect by studying the viscosity of **1**-**3** (Figure S30). In the condensed phase, the measured viscosity of these switches is invariant to the applied oscillator strain. The lowest viscosity was displayed by **1**-*Z* (1 Pa s), similar to that of glycerol, which we infer to improve the *E*/*Z* switching in the condensed phase. Compound **3** in both *E* and *Z* forms showed over 3 orders of magnitude higher conductivity than **1**, and the conductivity of compound **2** was ca. 20-40 times higher than **1**. The significant differences between the measured viscosities and conductivities of neat switches **1-3**, paired with their electrochemical properties in the solution state, allowed these relative contributions on electrochemical switching in the condensed phase to be decoupled.

Electrochemical switching in the devices was induced by applying a fixed cell potential of 1.77 V, a potential that results in a facile *Z* to *E* switching without causing any detectable degradation of the material (Figure S31). The extent of *Z* to *E* switching was determined at several time points using solution-state ^{1}H NMR following the dissolution of the film (Figure 3b). No degradation was observed over the course of the applied potential, indicating a clean redox initiated switching process. To evaluate the degree of possible Joule heating and consequent thermal reversion of *Z* isomers, we monitored the temperature of the film, using an IR thermometer, which did not exceed room temperature during the period of electrical poling. In addition, compounds **1-3** are exceptionally resistant to the thermally activated *Z* to *E* switching due to the high activation barriers, which was determined computationally (Section 3.4 of Supporting Information), and experimentally for **2** and **3**, to be between 114-123 kJ/mol (Figure 1c, Figure S14, S16). Holding a film of **3** at 80 °C for 1 h resulted in an 8% decrease, from 98% to 90%, of the *Z* isomer. We therefore infer that the observed switching in our devices under an applied electric field occurs electrochemically rather than thermally. We infer that charge neutrality is maintained in the system by reduction of the radical cations at the cathode and the generation of radical anions at the cathode (Figure S17 and S34).

After poling the devices at 1.77 V for 20 h, **3** displayed an 80% change in the %*Z*, whilst **1** achieved a 54% change and **2** showed a 14% change (Figure 3b). The rate in which charge is injected into films of **2** is significantly lower: 1.51 mC is injected into **3** after 3.6 min, whilst it takes 5 h to inject 1.51 mC into **2**, which is consistent with the lower conductivity of **2** compared to **3**. Given that the rate of *Z* to *E* isomerization of films of **2** under photoexcitation is also the lowest among the series of compounds, (Figure S32), we attribute the limited electrochemical switching of **2** to its high viscosity and the limited conformational change in the condensed phase, in addition to the low current level in its films (Figure S28, S30). Films comprised of **1** crystallized after approximately 2 hours of the potential being applied, induced by the increase in the composition of **1**-*E*, and was accompanied by a 75% reduction in the current. We attribute the gradually decreasing rate of the redox-initiated switching to the changes in the morphology of the film brought about during the crystallization process (Figure S33).[13] Visual inspection of the film revealed the presence of small voids in the crystallized film. We infer that these gaps limit the electroactive area of the device and increase the overall resistance. Both the formation of crystallization-induced voids in the film and a reduction in the intrinsic conductivity[42] (Table S7) of the photoswitches contribute to the increased resistance, thus reducing the completeness of electrochemical switching in the condensed phase.

The high completeness of switching achieved for **3** compared to **1** in films can be further rationalized by considering the redistribution of ions under an electric field, similar to the effect observed in light-emitting electrochemical cells.[43] Upon applying the electric field, the ions migrate to the corresponding electrode, creating surface-charge-dipole (SCD) regions. These SCD regions result in creating ohmic contacts at the ITO/photoswitch interface, improving the charge injection into the material.[44] Such behavior results in a greater number of charges being injected into **3** (51.0 mC over 5 h) than **1** (3.09 mC over 5 h) and therefore a greater degree of redox-induced switching. Thus, the combination of the stable ionic liquid phase of compound **3,** in both *E* and *Z* forms, and the absence of unfavorable crystallization, which increases the resistance across the film, are attributed to the high completeness of switching in the condensed phase.

Efficiency of Electrocatalytic Switching: Condensed Phase. The efficiency of redox-induced *Z* to *E* switching was enhanced in the condensed phase, as shown in Figure 3c. Photoswitch **1** showed the greatest efficiency requiring only 0.7 %mol of charge to achieve conversion, whereas switch **3** required 12.6 mol% of charge to achieve the same degree of switching. The high efficiency of reversion exhibited by **1** can be attributed to its lower conductivity compared to switch **3**. Indeed, we observe a trend, as the conductivity of the switch increases **1**<**2**<**3** (Table S7) the percentage of charges required for reversion increases (Figure 3c). In the case of switch **3,** the improved charge injection originating from the ionic migration, the higher mobility of electrons through the ionic liquid phase, and their favorable conduction through the cationic moieties of the molecule may incur the loss of charges to processes other than *Z* to *E* isomerization.

To determine the chemical stability under bias and cyclability, switches **1** and **3** were exposed to UV for 1 hour then 1.77 V for 20 hours at room temperature for five cycles (Figure S35-37). To demonstrate faster *Z* to *E* reversion and extended cyclability, switch **3** was exposed to 1.77V for 15 min at 80 °C and UV for 1 hour at room temperature for 20 cycles, and monitored by UV-vis spectroscopy (Figure S35). Over 20 cycles, the efficacy of electrochemical *Z* to *E* reversion was reduced from 100% to 22%, primarily due to the conductivity loss of the ITO slides over the repeated use (Figure S36). Only 2% degradation of the switch **3** was measured by NMR after 20 cycles.

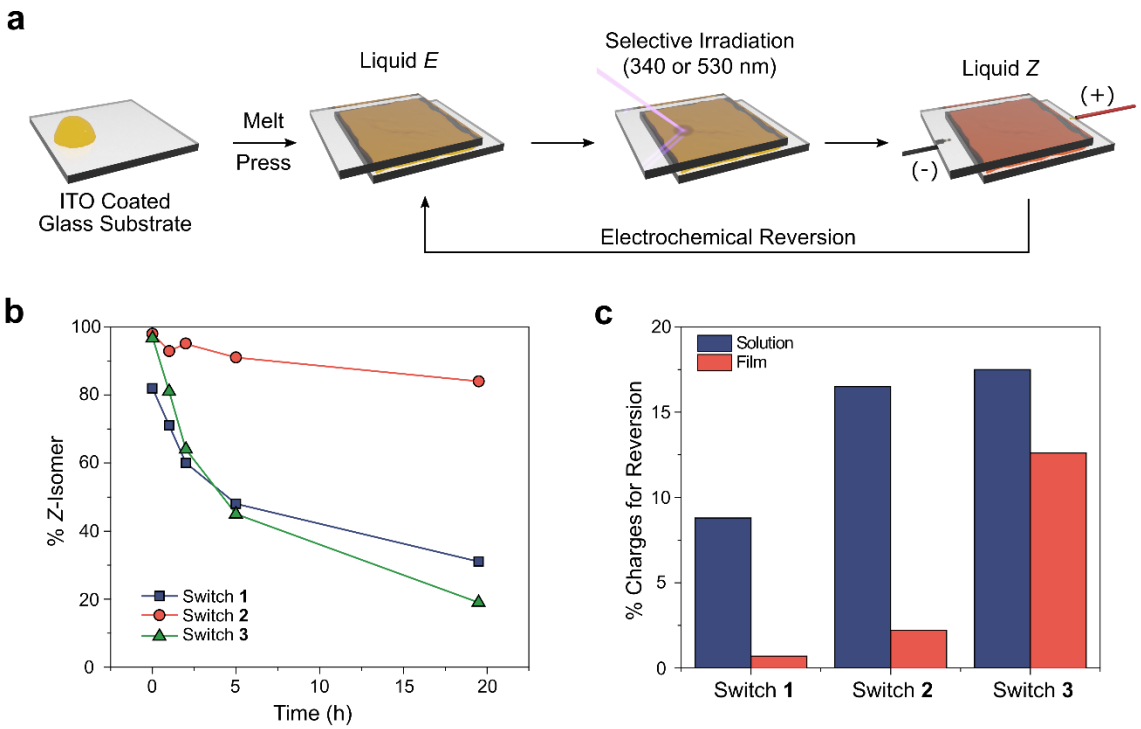


Figure 3. a, Schematic of the device fabrication process showing the *E* to *Z* photochemical isomerization and *Z* to *E* electrochemical reversion. **b,** The *Z* to *E* electrochemical reversion of switches **1-3** under 1.77 V exposure at room temperature in condensed phases. The films were prepared and sealed in the glovebox under an N_2 atmosphere to maintain a controlled and reproducible atmosphere. After the switching experiment, the films were dissolved to determine the %*Z*-isomer using ^{1}H NMR. Each data point corresponds to an individual experimental result obtained with a freshly prepared device. **c**, Comparison of percentage of electrons required for reversion in solution (blue bar) and the condensed phase (red bar).

We also compared the energy conversion efficiency (ECE) of switches **1-3** obtained by the photochemical vs. electrochemical triggering method. The optically induced *Z* to *E* isomerization under 395 nm results in an ECE of 4.7, 1.8, and 1.4% for switches **1**-**3**, respectively (Section 5 of the Supporting Information). For compounds **1** and **3** that display efficient electrochemical switching, we observe an improved ECE of 5.4 and 3.3%, respectively, demonstrating the advantage of using electrochemical triggering over the optical counterpart. The ECE of switch **2** that isomerizes poorly under electrical bias was determined to be 0.7%. The efficiencies were calculated using the quantum yields of *E* to *Z* and *Z* to *E* switching that we measured via actinometry (Section 2.23 of the Supporting Information) as well as the energy storage densities of switches **1**-**3:** 77, 31, and 25 kJ/mol, respectively, determined by differential scanning calorimetry. A comparison of MOST systems to other conventional energy storage and conversion systems is provided in Section 4 of the Supporting Information.

Elucidation of Design Rules. Taken together, we elucidate the following design rules to drive further improvements in the electrochemically triggered heat release from MOST materials. The steric hindrance experienced by a switch during *E/Z* isomerization in the condensed phase is reduced for materials with low viscosity (Figure S30). Switches that display liquid *E* and *Z* states are desirable for thin-film applications as they prevent phase separation and limit changes in conductivity induced during crystallization, both of which can significantly limit the redox-induced switching efficiency and completeness in the condensed phase. The films detailed in this work that exhibit a low conductivity afford the highest electrocatalytic switching efficiency, provided that the films are in a 10-25 µm thickness range. This is rationalized based on the ohmic contacts formed in the case of **3,** allowing a greater number of charges to be injected into the film per unit time, thus reducing the electrocatalytic efficiency. In contrast, the lower conductivity expressed by **1** reduces the number of charges injected per unit time, but these charges experience a greater turnover in the electrocatalytic switching process.

In summary, switches that exist as a liquid in both isomeric forms display the best electrochemical switching ability in the condensed phase. Those that are ionic liquids display more complete *Z* to *E* redox-induced switching at a cost of lower electrocatalytic efficiency. Switches prone to crystallization displayed a lower completeness of switching paired with a higher electrocatalytic efficiency. For applications requiring a high-power output (such as defrosting windshields), charged switches are arguably better suited. In instances where an energy-efficient release of thermal energy is desired, (smart climate control of home or greenhouse), the non-ionic liquid derivatives could be employed.

Conclusions

We have demonstrated that azoheteroarenes undergo electrocatalytic *Z* to *E* isomerization in both the solution and condensed phase; the efficiency of this chain reaction is improved at higher concentrations of photoswitch, and by over an order of magnitude in the condensed phase. Quantitative *Z* to *E* switching is observed for switches **1**-**3** in solution, however, only complete switching is observed for **3** in the condensed phase. This is attributed to its liquid *Z* and *E* isomeric forms.

The ability to trigger complete *Z* to *E* switching with a substoichiometric amount of charge in the condensed phase is attractive for MOST applications whereby a relatively small input of energy is required to trigger the release of the stored energy. Furthermore, the use of the electrocatalytic mechanism appears to be general in bypassing issues with poor photoconversion of *Z* to *E* switching, reducing the number of photochemically-orientated design specifications that need to be synthetically tuned. Further work is required before electrochemically triggered systems can compete in applications requiring rapid energy release. We anticipate that the rate of electrochemically induced isomerization could be further increased following several independent strategies: optimization of the chemical structure (improved charge transfer efficiency, lower thermal half-lives); adjustment of operating conditions (devices could be operated at elevated temperatures); tuning the device architecture (interdigitated electrodes to maximize the active area).

Alternatively, the combination of photochemical and electrochemical switching may be employed in a single device. Light could be exploited to trigger a fast heat release, while switching triggered electrochemically delivers a more sustained heat release, converting the remaining *Z*-isomers over a longer period. With further optimization, the redox-induced strategy detailed herein will undoubtedly be useful in the development of the next generation of MOST materials.

ASSOCIATED CONTENT

Supporting Information

The Supporting Information is available free of charge on the ACS Publications website.

Additional experimental details, materials, and methods, computational data and supplementary discussion of MOST systems (PDF)

AUTHOR INFORMATION

Corresponding Authors

*gracehan@brandeis.edu
*m.fuchter@imperial.ac.uk

Notes

The authors declare no competing financial interests.

ACKNOWLEDGMENT

We would like to acknowledge the Engineering and Physical Sciences Research Council (EP/R00188X/1), the Leverhulme Trust (RPG-2018-051) for funding. G.G.D.H. acknowledges Brandeis NSF MRSEC, Bioinspired Soft Materials (DMR-2011486), the SPROUT award (2019–042) from Brandeis Office of Technology Licensing, and Provost Research Award from Brandeis University. We thank Prof. Judith Herzfeld and Prof. Bruce Foxman at Brandeis University for their generous donation of a potentiostat and optical microscopes that were used in this research. We also thank Prof. Bing Xu and Adrianna Shy for helpful guidance on the rheometry experiments.

REFERENCES

(1) Dong, L.; Feng, Y.; Wang, L.; Feng, W. Azobenzene-Based Solar Thermal Fuels: Design, Properties, and Applications. *Chem. Soc. Rev.* **2018**, *47* (19), 7339–7368.

(2) Orrego-Hernández, J.; Dreos, A.; Moth-Poulsen, K. Engineering of Norbornadiene/Quadricyclane Photoswitches for Molecular Solar Thermal Energy Storage Applications. *Acc. Chem. Res.* **2020**, *53* (8), 1478–1487.

(3) Mansø, M.; Petersen, A. U.; Wang, Z.; Erhart, P.; Nielsen, M. B.; Moth-Poulsen, K. Molecular Solar Thermal Energy Storage in Photoswitch Oligomers Increases Energy Densities and Storage Times. *Nat. Commun.* **2018**, *9* (1), 1–7.

(4) Lorenz, P.; Hirsch, A. Photoswitchable Norbornadiene–Quadricyclane Interconversion Mediated by Covalently Linked C 60. *Chem. – A Eur. J.* **2020**, *26* (23), 5220–5230.

(5) Luchs, T.; Lorenz, P.; Hirsch, A. Efficient Cyclization of the Norbornadiene-Quadricyclane Interconversion Mediated by a Magnetic [Fe 3 O 4 −CoSalphen] Nanoparticle Catalyst. *ChemPhotoChem* **2020**, *4* (1), 52–58.

(6) Lorenz, P.; Luchs, T.; Hirsch, A. Molecular Solar Thermal Batteries through Combination of Magnetic Nanoparticle Catalysts and Tailored Norbornadiene Photoswitches. *Chem. – A Eur. J.* **2021**, *27* (15), 4993–5002.

(7) Wang, Z.; Udmark, J.; Börjesson, K.; Rodrigues, R.; Roffey, A.; Abrahamsson, M.; Nielsen, M. B.; Moth-Poulsen, K. Evaluating Dihydroazulene/Vinylheptafulvene Photoswitches for Solar Energy Storage Applications. *ChemSusChem* **2017**, *10* (15), 3049–3055.

(8) Zhitomirsky, D.; Cho, E.; Grossman, J. C. Solid-State Solar Thermal Fuels for Heat Release Applications. *Adv. Energy Mater.* **2016**, *6* (6), 1502006.

(9) Han, G. G. D.; Li, H.; Grossman, J. C. Optically-Controlled Long-Term Storage and Release of Thermal Energy in Phase-Change Materials. *Nat. Commun.* **2017**, *8* (1), 1446.

(10) Cho, E. N.; Zhitomirsky, D.; Han, G. G. D.; Liu, Y.; Grossman, J. C. Molecularly Engineered Azobenzene Derivatives for High Energy Density Solid-State Solar Thermal Fuels. *ACS Appl. Mater. Interfaces* **2017**, *9* (10), 8679–8687.

(11) Kanai, Y.; Srinivasan, V.; Meier, S. K.; Vollhardt, K. P. C.; Grossman, J. C. Mechanism of Thermal Reversal of the (Fulvalene)Tetracarbonyldiruthenium Photoisomerization: Toward Molecular Solar-Thermal Energy Storage. *Angew. Chem. Int. Ed.* **2010**, *49* (47), 8926–8929.

(12) Gerkman, M. A.; Han, G. G. D. Toward Controlled Thermal Energy Storage and Release in Organic Phase Change Materials. *Joule* **2020**, *4* (8), 1621–1625.

(13) Gerkman, M. A.; Gibson, R. S. L.; Calbo, J.; Shi, Y.; Fuchter, M. J.; Han, G. G. D. Arylazopyrazoles for Long-Term Thermal Energy Storage and Optically Triggered Heat Release below 0 °C. *J. Am. Chem. Soc.* **2020**, *142* (19), 8688–8695.

(14) Calbo, J.; Weston, C. E.; White, A. J. P. P.; Rzepa, H. S.; Contreras-García, J.; Fuchter, M. J. Tuning Azoheteroarene Photoswitch Performance through Heteroaryl Design. *J. Am. Chem. Soc.* **2017**, *139* (3), 1261–1274.

(15) Bléger, D.; Schwarz, J.; Brouwer, A. M.; Hecht, S. O -Fluoroazobenzenes as Readily Synthesized Photoswitches Offering Nearly Quantitative Two-Way Isomerization with Visible Light. *J. Am. Chem. Soc.* **2012**, *134* (51), 20597–20600.

(16) Calbo, J.; Thawani, A. R.; Gibson, R. S. L.; White, A. J. P.; Fuchter, M. J. A Combinatorial Approach to Improving the Performance of Azoarene Photoswitches. *Beilstein J. Org. Chem.* **2019**, *15*, 2753–2764.

(17) Zhang, Z.-Y.; He, Y.; Wang, Z.; Xu, J.; Xie, M.; Tao, P.; Ji, D.; Moth-Poulsen, K.; Li, T. Photochemical Phase Transitions Enable Coharvesting of Photon Energy and Ambient Heat for Energetic Molecular Solar Thermal Batteries That Upgrade Thermal Energy. *J. Am. Chem. Soc.* **2020**, *142* (28), 12256–12264.

(18) Samanta, S.; Beharry, A. A.; Sadovski, O.; McCormick, T. M.; Babalhavaeji, A.; Tropepe, V.; Woolley, G. A. Photoswitching Azo Compounds in Vivo with Red Light. *J. Am. Chem. Soc.* **2013**, *135* (26), 9777–9784.

(19) Konrad, D. B.; Savasci, G.; Allmendinger, L.; Trauner, D.; Ochsenfeld, C.; Ali, A. M. Computational Design and Synthesis of a Deeply Red-Shifted and Bistable Azobenzene. *J. Am. Chem. Soc.* **2020**, *142* (14), 6538–6547.

(20) Shi, Y.; Gerkman, M. A.; Qiu, Q.; Zhang, S.; Han, G. G. D. Sunlight-Activated Phase Change Materials for Controlled Heat Storage and Triggered Release. *J. Mater. Chem. A* **2021**, *9* (15), 9798–9808.

(21) Corruccini, R. J.; Gilbert, E. C. The Heat of Combustion of Cis - and Trans -Azobenzene. *J. Am. Chem. Soc.* **1939**, *61* (10), 2925–2927.

(22) Gurke, J.; Quick, M.; Ernsting, N. P.; Hecht, S. Acid-Catalysed Thermal Cycloreversion of a Diarylethene: A Potential Way for Triggered Release of Stored Light Energy? *Chem. Commun.* **2017**, *53* (13), 2150–2153.

(23) Wang, Z.; Losantos, R.; Sampedro, D.; Morikawa, M.; Börjesson, K.; Kimizuka, N.; Moth-Poulsen, K. Demonstration of an Azobenzene Derivative Based Solar Thermal Energy Storage System. *J. Mater. Chem. A* **2019**, *7* (25), 15042–15047.

(24) Weston, C. E.; Richardson, R. D.; Haycock, P. R.; White, A. J. P.; Fuchter, M. J. Arylazopyrazoles: Azoheteroarene Photoswitches Offering Quantitative Isomerization and Long Thermal Half-Lives. *J. Am. Chem. Soc.* **2014**, *136* (34), 11878–11881.

(25) Knie, C.; Utecht, M.; Zhao, F.; Kulla, H.; Kovalenko, S.; Brouwer, A. M.; Saalfrank, P.; Hecht, S.; Bléger, D. Ortho -Fluoroazobenzenes: Visible Light Switches with Very Long-Lived Z Isomers. *Chem. Eur. J.* **2014**, *20* (50), 16492–16501.

(26) Goulet-Hanssens, A.; Rietze, C.; Titov, E.; Abdullahu, L.; Grubert, L.; Saalfrank, P.; Hecht, S. Hole Catalysis as a General Mechanism for Efficient and Wavelength-Independent Z → E Azobenzene Isomerization. *Chem* **2018**, *4* (7), 1740–1755.

(27) Goulet-Hanssens, A.; Utecht, M.; Mutruc, D.; Titov, E.; Schwarz, J.; Grubert, L.; Bléger, D.; Saalfrank, P.; Hecht, S.; Bléger, D. B.; et al. Electrocatalytic Z → E Isomerization of Azobenzenes. *J. Am. Chem. Soc.* **2016**, *139* (1), 335–341.

(28) Waidhas, F.; Jevric, M.; Bosch, M.; Yang, T.; Franz, E.; Liu, Z.; Bachmann, J.; Moth-Poulsen, K.; Brummel, O.; Libuda, J. Electrochemically Controlled Energy Release from a Norbornadiene-Based Solar Thermal Fuel: Increasing the Reversibility to 99.8% Using HOPG as the Electrode Material. *J. Mater. Chem. A* **2020**, *8* (31), 15658–15664.

(29) Brummel, O.; Waidhas, F.; Bauer, U.; Wu, Y.; Bochmann, S.; Steinrück, H.-P.; Papp, C.; Bachmann, J.; Libuda, J. Photochemical Energy Storage and Electrochemically Triggered Energy Release in the Norbornadiene–Quadricyclane System: UV Photochemistry and IR Spectroelectrochemistry in a Combined Experiment. *J. Phys. Chem. Lett.* **2017**, *8* (13), 2819–2825.

(30) Brummel, O.; Besold, D.; Döpper, T.; Wu, Y.; Bochmann, S.; Lazzari, F.; Waidhas, F.; Bauer, U.; Bachmann, P.; Papp, C.; et al. Energy Storage in Strained Organic Molecules: (Spectro)Electrochemical Characterization of Norbornadiene and Quadricyclane. *ChemSusChem* **2016**, *9* (12), 1424–1432.

(31) Gassman, P. G.; Hershberger, J. W. An Electrochemical "Switch" for Starting and Stopping the Energy-Releasing Conversion of Quadricyclanes to Norbornadienes. *J. Org. Chem.* **1987**, *52* (7), 1337–1339.

(32) Gelebart, A. H.; Jan Mulder, D.; Varga, M.; Konya, A.; Vantomme, G.; Meijer, E. W.; Selinger, R. L. B.; Broer, D. J. Making Waves in a Photoactive Polymer Film. *Nature* **2017**, *546* (7660), 632–636.

(33) Zha, R. H.; Vantomme, G.; Berrocal, J. A.; Gosens, R.; de Waal, B.; Meskers, S.; Meijer, E. W. Photoswitchable Nanomaterials Based on Hierarchically Organized Siloxane Oligomers. *Adv. Funct. Mater.* **2018**, *28* (1), 1703952.

(34) Kulkarni, C.; Curvers, R. H. N.; Vantomme, G.; Broer, D. J.; Palmans, A. R. A.; Meskers, S. C. J.; Meijer, E. W. Consequences of Chirality in Directing the Pathway of Cholesteric Helix Inversion of Π-Conjugated Polymers by Light. *Adv. Mater.* **2021**, *33* (2), 2005720.

(35) Leith, G. A.; Martin, C. R.; Mathur, A.; Kittikhunnatham, P.; Park, K. C.; Shustova, N. B. Dynamically Controlled Electronic Behavior of Stimuli-Responsive Materials: Exploring Dimensionality and Connectivity. *Adv. Energy Mater.* **2021**, *2100441*, 2100441.

(36) Williams, D. E.; Martin, C. R.; Dolgopolova, E. A.; Swifton, A.; Godfrey, D. C.; Ejegbavwo, O. A.; Pellechia, P. J.; Smith, M. D.; Shustova, N. B. Flipping the Switch: Fast Photoisomerization in a Confined Environment. *J. Am. Chem. Soc.* **2018**, *140* (24), 7611–7622.

(37) Gonzalez, A.; Kengmana, E. S.; Fonseca, M. V.; Han, G. G. D. Solid-State Photoswitching Molecules: Structural Design for Isomerization in Condensed Phase. *Mater. Today Adv.* **2020**, *6*, 100058.

(38) Rice, A. M.; Martin, C. R.; Galitskiy, V. A.; Berseneva, A. A.; Leith, G. A.; Shustova, N. B. Photophysics Modulation in Photoswitchable Metal–Organic Frameworks. *Chem. Rev.* **2020**, *120* (16), 8790–8813.

(39) Morikawa, M.; Yang, H.; Ishiba, K.; Masutani, K.; Hui, J. K.-H.; Kimizuka, N. A Liquid Arylazopyrazole Derivative as Molecular Solar Thermal Fuel with Long-Term Thermal Stability. *Chem. Lett.* **2020**, *49* (6), 736–740.

(40) Ishiba, K.; Morikawa, M.; Chikara, C.; Yamada, T.; Iwase, K.; Kawakita, M.; Kimizuka, N. Photoliquefiable Ionic Crystals: A Phase Crossover Approach for Photon Energy Storage Materials with Functional Multiplicity. *Angew. Chem. Int. Ed.* **2015**, *54* (5), 1532–1536.

(41) Kolivoška, V.; Gál, M.; Lachmanová, Š.; Valášek, M.; Hromadová, M.; Pospíšil, L. Spectroelectrochemical Determination of the Electron Consumption. *Anal. Chim. Acta* **2011**, *697* (1–2), 23–26.

(42) Nguyen, D. T.; Freitag, M.; Gutheil, C.; Sotthewes, K.; Tyler, B. J.; Böckmann, M.; Das, M.; Schlüter, F.; Doltsinis, N. L.; Arlinghaus, H. F.; et al. An Arylazopyrazole-Based N-Heterocyclic Carbene as a Photoswitch on Gold Surfaces: Light-Switchable Wettability, Work Function, and Conductance. *Angew. Chem. Int. Ed.* **2020**, *59* (32), 13651–13656.

(43) Schlingman, K.; Chen, Y.; Carmichael, R. S.; Carmichael, T. B. 25 Years of Light-Emitting Electrochemical Cells: A Flexible and Stretchable Perspective. *Adv. Mater.* **2021**, *33* (21), 2006863.

(44) Greenfield, J. L.; Di Nuzzo, D.; Evans, E. W.; Senanayak, S. P.; Schott, S.; Deacon, J. T.; Peugeot, A.; Myers, W. K.; Sirringhaus, H.; Friend, R. H.; et al. Electrically Induced Mixed Valence Increases the Conductivity of Copper

Helical Metallopolymers. *Adv. Mater.* **2021**, *33* (24), 2100403.

TOC Graphic

